Optical processor for the very large array (VLA) radiotelescope: system concept

I.Cindrich, C. C. Aleksoff, J. R. Fienup, L. E. Somers*
Radar and Optics Division, Environmental Research Institute of Michigan
P.O. Box 8618, Ann Arbor, Michigan 48107

Abstract

Optical Fourier transform processing of radiotelescope visibility function data is reviewed. Emphasis is placed on the aspects of the processor design that arise from the unusual characteristics of the data. The complex visibility function is available only over a partially filled aperture consisting of a set of elliptical paths. It is recorded at the input to the optical processor on a carrier frequency as a real nonnegative transmittance. Since a bipolar sky brightness function output is to be computed, the output of the optical Fourier transform channel is mixed with a reference beam and the difference is taken of two successive measurements differing in reference phase by 180°. Experimental results demonstrating processor concepts are shown and a processor system design approach is described.

Introduction

Basic to radio astronomy is the determination of the distribution of radiated power from celestial sources with the radiotelescope. This power distribution or sky brightness, B, is a measure of the power per unit solid angle for the temporal frequency band under observation. The sky brightness data obtained serves a primary role in the scientific research on the physics of celestial bodies.

Over the past few decades, radiotelescopes have evolved from radio receivers of modest performance having simple antennas of limited angular resolution to present day receivers of high sensitivity and stability, with fine angular resolution obtained by synthetic aperture antenna concepts. These systems utilize a ground-based large array antenna with array elements operated as interferometer pairs. As the antenna array moves, due to earth's rotation, an extensive received signal history is collected from which a high resolution receiving aperture is synthesized.

As an example, the very large array radiotelescope (VLA) currently under development near Soccorro, New Mexico, by the National Radio Astronomy Observatory (NRAO) employs the aperture synthesis concept. This VLA will make use of up to 27 ground-based antenna elements; each element being a steerable 25 meter diameter parabolic dish located along the arms of a wye-shaped array pattern. Four basic array arrangements (A, B, C, D) are planned which are denoted according to a ground distance over which the array elements are spread. This system provides as its output a signal history called the visibility function V. It is related to the desired measure of the sky brightness function B through the Fourier transform. Thus, Fourier transform processing of the radiotelescope output V allows recovery of a measured version of B.

We will describe a design concept for an optical Fourier transform processor system for radiotelescope visibility function data, starting first with a review of sky brightness image and visibility function properties and then going on to a processor configuration and supporting experimental data.

Sky brightness

The sky brightness[1,2] can be taken as a two-dimensional spatial distribution B(x, y) for the purposes of this discussion. The x and y variables define orthogonal position coordinates relative to a fixed reference direction within the field of observation of the radiotelescope. B(x, y) has physical units of power per unit area and per unit solid angle for the location (x, y). It is a real valued function and its spatial variation encompasses point-like (stars) as well as highly dispersed distributions. The magnitude of the brightness function must be generated with an accuracy of one per cent of its peak value or better. An example of sky brightness map data is shown in Figure 1.

*L.E. Somers is with the Lawrence Livermore Laboratory, Livermore, California 94550.

Visibility function

The measured visibility function V, available at the radiotelescope system output, is a composite of signals associated with the antenna array elements. We will discuss some of the salient properties of V pertinent to its processing. The derivation of V is described in the literature[1,2]. The NRAO/Soccorro system concept will be used as a basis for our discussion. Each signal of the visibility function composite is derived from correlation processing of the reception from selected pairs of antennas of the 27 element array. Correlation is performed over a succession of short time intervals thus causing V to be a sampled function. Signals from 351 antenna pairs, i.e., $n(n-1)/2$ for $n = 27$, which are derived simultaneously in parallel channels of the radiotelescope system constitute V. The time history of V corresponds to the movement of the antenna array due to the earth's rotation. Typically during the observation interval over which the visibility function is being collected, data is accumulated in buffer storage. It is then read out of buffer storage over a short time interval for Fourier transform processing to generate the sky-brightness map B. The broad temporal bandwidth of the radiotelescope can be divided into as many as 256 individual narrow spectral bands or lines with a visibility function generated for each line. Fewer bands of broader bandwidth, about eight, may also be generated and are referred to as the continuum case. In the following, the description of the visibility function processing applies to each individual spectral line. Each spectral line is processed separately.

As will be explained in greater detail below, the visibility function may be considered as a time varying signal or as a spatially varying signal defined in a (u, v) spatial domain. A simulated example of the elliptical paths on which V(u, v) is measured is shown in Figure 2 where each individual signal, of the total composite of 351 signals which make up V, occurs along one of the curved paths shown.

The ratio of the maximum value to the minimum value (noise) of the magnitude of V will be about 10:1 for about two-thirds of the spectral line visibility functions expected. Normally the remaining third of the expected visibility functions will have a ratio of about 100:1. The space-bandwidth product of V for the A-array over a viewing field extending to the -3 dB width of the beam pattern for an individual array element is 3000 in each of its two dimensions.

The time domain representation of the visibility function will be written as

$$V(t_n) = \sum_{k=1}^{351} V_k(t_n) \tag{1}$$

where k identifies an antenna element pair of a particular baseline (separation) length and t_n the n-th discrete sample of the continuous succession of equally spaced samples in each V_k.

More appropriate to the Fourier transform processing to be performed on V is the spatial domain representation of the visibility function, V(u, v), which we can write as

$$V(u_n, v_n) = \sum_{k=1}^{351} V_k(u_n, v_n) \tag{2}$$

The variables u, v have the form of a distance normalized by the operating wavelength of the radiotelescope. More specifically, the radiotelescope spatial domain related to u and v is a plane that is normal to the reference pointing direction of the radiotelescope. Defining orthogonal coordinate unit vectors $\hat{u}$ and $\hat{v}$ in this plane, we have u as the normalized component of an antenna baseline in the u direction, and similarly for v.

As noted previously, the signal history of the visibility function in the spatial domain falls along a set of elliptical paths (or tracks), one path for each of the 351 baselines (antenna pairs). These u, v plane paths are well defined in terms of the earth's rotational angle (hour angle h), the declination angle of the reference pointing direction of the radiotelescope (δ), the latitude angle of the antenna site location (ℓ), and the east-west and south-north component lengths of the antenna baseline at the earth's surface (B_{EW} and B_{SN}). Operating wavelength is λ. Path coordinates in the u, v plane are given by the following expressions.

$$\lambda u = B_{EW} \cos h + B_{SN} \sin \ell \sin h \tag{3}$$

$$\lambda v = -B_{EW} h \sin h \sin \delta + B_{SN} \sin \ell \cos h \sin \delta + B_{SN} \cos \ell \cos \delta \tag{4}$$

The locus of the u- v points as a function of time (or hour angle h) will in general be an ellipse. Solving the above expressions for $(\lambda u)^2 + (\lambda v)^2$ allows formulation of the equation for the elliptical path, i.e.,

$$\frac{(\lambda u)^2}{B_{EW}^2 + B_{SN}^2 \sin^2 \ell} + \frac{(\lambda v - B_{SN} \cos \ell \cos \delta)^2}{\sin^2 \delta \left(B_{EW} + B_{SN} \sin^2 \ell\right)} = 1 \tag{5}$$

The ellipse has the following parameters

u major axis: $\left[B_{EW}^2 + B_{SN}^2 \sin^2 \ell\right]^{1/2}$

v minor axis: $\left[\sin^2 \delta \left(B_{EW}^2 + B_{SN}^2 \sin^2 \ell\right)\right]^{1/2}$

center at: $\lambda u = 0$

$\lambda v = B_{SN} \cos \ell \cos \delta$

Note that the elliptical paths can have the degenerate forms of circles when $\delta = \pi/2$ and lines when $\delta = 0$.

In the simulated example of the visibility function of Figure 2, the elliptical paths along which this function lies are quite evident. It will be useful to recognize the elliptical tracks themselves as an aperture or mask function having a finite track width. The amplitude and phase variation of the visibility function V occurs within this aperture function, varying along the track length.

The visibility function made available for processing will be complex valued, i.e.,

$$V(t_n) = |V(t_n)| \, e^{j\phi(t_n)} \tag{6}$$

or

$$V(u_n, v_n) = |V(u_n, v_n)| \, e^{j\phi(u_n, v_n)} \tag{7}$$

More specifically, the values for the complex visibility function in phase and quadrature (real and imaginary) parts, $V_i(u_n, v_n)$ and $V_q(u_n, v_n)$ and the corresponding position coordinates (u_n, v_n) would be provided in digital form at the radiotelescope output buffer store. It is placed into storage as a sample sequence natural to the manner in which it is generated. At each time t_n, 351 data points (one for each baseline) are entered into storage. Note that for any one time t_n, the corresponding u, v plane locations, which are known, will in general be different since u and v are dependent on relative baseline length and geometric location which changes as the earth rotates. It should be noted that the complex visibility function will be Hermitian since B is real, i.e., $V(u, v) = V^*(-u, -v)$.

When the visibility function is read out of buffer storage to be made available for Fourier transform post processing, the sequence often preferred is either along a common time sample or along baselines. A third possibility is defined in terms of the u v position coordinates of the visibility function. It is a raster sequence in which data is read out over adjacent lines of constant u (or v). Generating the raster format would require extensive reformatting of the visibility data samples.

Optical processing for Fourier transformation will require conversion of the visibility function to a form suited to use as the input to an optical channel. As one example, we can use a real signal which is placed on a carrier frequency w for phase preservation and on a bias amplitude to assure preservation of the bipolar properties of V. An example of

this real signal format is given by the following expression which will be proportional to optical amplitude transmissivity (t) realizable in a film recording of the visibility function,

$$t(u, v) \sim \text{Bias} + |V(u, v)| \cos [wu + \phi(u, v)] \tag{8}$$

The above expression does not include an explicit statement of the aperture functions inherent in an optical recording of the visibility data. As noted previously, the visibility data occurs along elliptical tracks in the u-v domain and in an optical recording the tracks have a finite spatial distribution which we denote $A_t(u, v)$. In addition, the entire composite of the recorded data will fall within a bounded area which will be defined by a two-dimensional envelope or aperture function denoted $A(u, v)$. A more complete expression for optically recorded visibility function data which includes the aperture functions $A_t(u, v)$ and $A(u, v)$, along with their recorded bias levels b_t and b within these apertures, is given below.

$$t(u, v) \sim A(u,v)\left\{A_t(u, v) [b_t + |V(u, v)| \cos (wu + \phi(u, v))] + b[1 - A_t(u, v)]\right\} \tag{9}$$

Figure 3 depicts the nature of recorded visibility function data given by Equation 9.

Point source brightness function

The measured sky brightness for a single point source (star), obtained by Fourier transformation of the corresponding visibility function for that source, characterizes the impulse response of the total system (the radiotelescope and the FT processor). The point source visibility function is a linear grating fringe pattern seen through the $A_t(u, v)$ aperture defined by the composite of elliptical tracks shown before in Figure 2. The Fourier transform of this visibility function has a spatial distribution as shown in Figure 4 which is defined by the transform of the elliptical track aperture function. Its location is proportional to fringe frequency. This spatial distribution or impulse response is often called the synthetic or VLA beam.

Of the four antenna array configurations (A, B, C, D) for the NRAO Soccorro site, the 72 km A-array poses the most demanding requirements for processor performance because its visibility data has the largest space-bandwidth product of 3000 cycles. The B, C and D arrays are much less demanding with their reduced u, v plane sizes of 21.92 km, 6.67 km and 2.03 km and the correspondingly smaller space-bandwidth products of 912, 278 and 84.

Optical processing

An optical processor system for visibility function processing is comprised of an optical Fourier channel together with provisions for entering visibility data at its input and provisions for observing and removing sky brightness data at its output. The optical channel provides for the two dimensional Fourier transform operation.

Several optical processor system configurations are of course possible.[3,4] To illustrate, we consider the familiar case of a coherent optical channel in which the input data is illuminated with a convergent light wave as shown in Figure 5. The input data is assumed to be a spatial representation as can be accomplished with photographic film or with other materials or devices.

The Fourier relationship between the input and output plane of the optical processor is realized in terms of the "field" of the light beam. Since, as a practical matter, the light intensity rather than the light field is accessible for use at the processor output, the optical processing channel will provide the magnitude squared of the desired Fourier transform rather than the Fourier transform, per se. Simply detecting the squared magnitude and then taking the square root is not adequate, since the sky brightness function obtained has area of negative sidelobes. The desired Fourier transform can be obtained, however, by adding a reference light beam at the output plane, as shown in Figure 5. With this arrangement, the light intensity present at the processor output is the magnitude squared of the sum of reference and Fourier fields; this quantity contains a term proportional to the desired output.

This concept can be illustrated mathematically[5]. Consider the visibility function as the film recorded input data $t(u, v)$ at the processor input plane with illumination by the light wave $U_i(u, v)$. The expression for the light field passing through the input plane data is $U_i(u, v)t(u, v)$.

Assuming that the illuminating wave has constant amplitude at the input plane, we have at the output plane the optical Fourier transform field $U_1(x, y)$ which can be expressed as

$$U_1(x, y) = A_1 e^{j\theta_1(x,y)} F[t(u, v)]. \tag{10}$$

where $\theta_1(x, y)$ is a residual phase term which typically has quadratic variation with x and y and A_1 is essentially constant. The Fourier transform term F[t] has the explicit form

$$F\left[t(u, v)\right] = \int_{-\infty}^{\infty} t(u, v)\, e^{-j\frac{2\pi}{\lambda z}(xu+yv)}\, du\, dv. \tag{11}$$

Here z is the processor working focal length, λ the optical wavelength, and $x/\lambda z$ and $y/\lambda z$ are spatial frequency coordinates at the output plane of the optical channel.

Using a reference wave $U_2(x, y)$ of the form

$$U_2(x, y) = A_2 e^{j\theta_2(x,y)}, \tag{12}$$

the optical processing channel output light intensity distribution is

$$\begin{aligned} I(x, y) &= |U_1(x, y) + U_2(x, y)|^2 \\ &= 2A_1A_2F[t(u, v)] \cos(\theta_1 - \theta_2) + |U_1|^2 + |U_2|^2. \end{aligned}$$

The output of interest in the above expression is the Fourier transform F[t]. It is available multiplied by the constant $2A_1A_2$ and a function $\cos(\theta_1 - \theta_2)$, where $(\theta_1 - \theta_2)$ can have a prescribed phase. Of the undesired or extraneous terms, $|U_1|^2$ contains the modulus squared of F[t] and $|U_2|^2$ is the modulus squared of the reference wave. These extraneous terms are to be avoided. This is accomplished by a two step process in which we generate the output twice, each one differing by the value of the phase of $(\theta_1 - \theta_2)$, followed by subtraction of these two outputs. Denoting the output as $I_1(x, y)$ when $(\theta_1 - \theta_2) = 0$ and $I_2(x, y)$ when $(\theta_1 - \theta_2) = \pi$, then the difference $I_1 - I_2$ removes the extraneous terms and gives the desired sky brightness output B(x, y) as

$$\begin{aligned} B(x, y) &= I_1(x, y) - I_2(x, y) \\ &= 4A_1A_2F[t(u, v)] \end{aligned} \tag{14}$$

We realize the desired sky brightness image as one sideband (diffracted order)of the Fourier transform F[t] of the spatially recorded version of the visibility function V. This output can be converted to an electronic signal with a scanning photodetector and then digitized, thus providing digital sky brightness map data to the astronomer for computer analysis. The conjugate diffracted order provides an additional output which can be used as a direct immediate access display.

Companion papers[6,7] discuss in greater detail the topics of encoding and optical recording of the input visibility data[6] and accuracy of the Fourier transform operation[7].

Processing experiments

An experimental breadboard of the Fourier transform processing channel was assembled to demonstrate and verify the merit of the basic processing concept.

A diagram of the optical channel is shown in Figure 6. An after-the-lens input gate was used for entry of input data-film recordings. The input-to-output plane spacing or working focal length was 3.3 m. Illumination with a He-Ne laser beam (λ = 632.8 nm) was provided by focusing the laser beam onto a pinhole filter and then imaging the pinhole (point source) onto the output plane of the processor with a lens. A diverging spherical reference was used originating from a focal point located at the center of the input film plane. This wave was generated by collecting a small portion of the Fourier lens output beam with a separate smaller lens, which then focused the light to a point at the center of the input plane. The relative phase between the reference beam and the Fourier beam was shifted between 0 and π by changing the length of the optical path of the reference beam. This was accomplished by mounting a flat glass plate in the reference wave just before the reference wave lens. An electronic actuator rotated the plate between two positions of a slightly different angle which caused the reference wave to experience slightly different optical path lengths which were set to correspond to a phase of 0 and π relative to the Fourier beam. This change of phase was synchronized to the output photodetector scan period to allow readout at the brightness plane with two successive scans, which cor-

respond to the 0 and π phase condition. The two scans were then subtracted to obtain sky brightness data as discussed previously.

Sample input data for the processing experiments was generated with a precision CRT/film recorder system at ERIM. Recordings of simple sinusoidal rasters and also of simulated VLA data were made. Simulated VLA data of a point source was provided by the NRAO in the form of computer compatible magnetic tape recordings with the data in a raster format. These tapes were converted to analog electronic data with an appropriate bias level, carrier frequency and synchronization trigger pulses and then recorded on the CRT/film recorder using the ERIM special-purpose data-processing facilities.

A Reticon 1024 element linear photodetector array was used to scan the output sky-brightness plane. Scanning was done electronically along the length of the linear array and the array was moved mechanically in the direction perpendicular to the array length with a precision stepping motor and drive assembly. Data readout at the output plane was viewed on a special-purpose oscilloscope/scan recorder system and it was also digitized and recorded on magnetic tape for viewing on a Ramtek TV-type display which is part of an ERIM computer facility.

Examples of the experimental data obtained at the output of the breadboard optical channel are shown in Figures 7 and 8. Figure 7 shows the results (which do not include compensation of pattern defects in the photodetector) for a one-dimensional scan through the output obtained when the u, v plane input is a clear circular aperture. Data is shown for both single scans through the processor output (a) and for the difference of two scans (b), with the subtracted scans differing by the 0 and π phase change between reference and Fourier beams in the optical channel. Figure 8 gives similar uncompensated data for a synthetic beam at the processor output when the input u, v plane film data is a film recording of a simulated visibility function of a point source.

The data of Figures 7 and 8 both do not have photodetector defect compensation. In addition, the data of Figure 8 was obtained using a larger u, v plane aperture than that of Figure 7 and the modest quality of the breadboard processor over this larger aperture caused the nonsymmetric side-lobe error seen in Figure 8b.

Figure 9 shows a photograph of the sky-brightness plane data seen on the ERIM Ramtek display for the case of a clear square u, v plane input aperture. This data was obtained by a sequence of steps starting with photodetector readout of the processor sky-brightness output plane. Two successive readouts were made. Each was a two-dimensional scan obtained with the Reticon photodetector array. The outputs differed by the 0, π phase conditions within the optical channel of the processor. Each scanned output was digitized, recorded on magnetic tape and compensated for fixed-pattern variations caused by the photodetector. The magnetic tape data was then used as the input for a computer subtraction of the two scans (0, π) to give the desired sky-brightness data which was then displayed on a Ramtek (TV) display, as shown in Figure 8. For the purpose of display, a bias was added to the sky brightness data to make it everywhere nonnegative.

System design concept

A processor system[3] for VLA visibility function data, based on the optical Fourier transform computation described previously, will be comprised of an optical transform channel and provisions for three interfaces: input, output, and system control. Figure 10 provides a functional diagram for a system configuration employing film recorded visibilty function data at the optical channel input with output sky brightness data in the form of a direct analog display and also digital mag tape.

Visibility function data is made available from digital storage at the radiotelescope output. This output data is taken on a frame basis; that is, data for a single spectral line or band for $V(u_n, v_n)$ is read out of storage for recording on film. Prior to the film recording step, the visibility data must be properly formatted, converted to an analog signal, and placed on a carrier frequency and amplitude bias level. This is accomplished by the data formatter of Figure 10. The data formatter also serves to generate scan control signals for control of the optical recorder writing beam. The optical recorder is a CRT/film device which utilizes rapid automated chemical development of the film. Recording is accomplished one frame at a time, each film frame being handled in sequence by an automated film transport. The film frame progresses through recording (exposure), development and then entry at the optical channel input plane. After optical processing, the transport system removes the data frame (film) from the optical channel input and enters it into a storage file from which it can be retrieved for re-use by remote command. A 70 mm film size is used with the visibility data contained within a central 50 mm x 50 mm area. The largest expected space-bandwidth product of 3000 x 3000 would be recorded with a spatial bandwidth of 60 c/mm.

The optical Fourier transform channel consists of the Fourier transform lens, a liquid gate for input data (film frame) entry, provisions for output sky brightness data extraction, and the means for forming the two illuminating light beams (Fourier channel and reference beams). A diagram of the optical channel is provided in Figure 11. A 3.3 meter focal length Fourier transform lens with diffraction-limited performance for an input data frame having a 3000 x 3000 space bandwidth product would be suited to VLA data processing needs. The input data is illuminated with the converging wave generated by the Fourier lens with the output plane located 3 meters from the input plane. The reference wave enters the Fourier channel by reflection from a small area surface at the u = 0, v = 0 region. This is permissable since the radiotelescope does not collect data for this region of the u, v plane. The optical configuration used tends to minimize optical components between the input and output planes of the Fourier channel.

Two sky brightness images are available at the processor output plane as a normal consequence of having separated plus and minus diffracted waves at the output of a coherent optical channel. One output is scanned with a photodetector array, converted to digital form, and then used in the computation of the difference of 0 and π shifted outputs described previously. The resultant data is recorded on mag tape for later use by the astronomer. A linear photodetector array composite of 7,200 elements is used which is electronically scanned in one direction and mechanically transported over an equal number of samples in the orthogonal direction of the brightness image. The high sampling density is needed to minimize interpolation by the user of the output data. The second output image is observed through a high resolution TV camera whose output is displayed on a monitor at the system control console. This second image is provided at the processor output without the reference wave since the modulus squared of the sky brightness is adequate for quick access viewing by the operator at the system control console.

The output plane of the optical processor will be capable of about 1500 x 1500 beam (null to null) diameters corresponding to the diffraction-limited output for the 50 mm x 50 mm input aperture. However, the maximum number of synthesized VLA beams at the optical processor output will be lower since a VLA beam results from a relatively sparsely filled input data aperture described by the 351 elliptical tracks. A maximum of about 800 VLA beam diameters (null to null) is expected for the A array configuration and fewer for the B, C, and D configurations.

If we include the response properties of the total processor system from the optical recorder to the photodetector output, the sky brightness data will have the form

$$B(x, y) = 4A_1A_2k_rk_d\, F[t(u, v)]G_r(x, y) \otimes g_d(x, y)\, \overline{III}\left(\frac{x}{d_x}\right) \overline{III}\left(\frac{y}{d_y}\right) \qquad (15)$$

where $\otimes$ denotes convolution. The output is scaled by $4A_1A_2k_rk_d$ which now includes the optical recorder gain k_r and photodetector gain k_d. It is also weighted by the recorder frequency response function G_r, smoothed by the photodetector spatial response function g_d and sampled by the photodetector as indicated by the sampling functions $\overline{III}$, with sampling periods d_x and d_y.

Overall control of the processor system is provided from a central control console having terminal keyboard access and a TV monitor for sky brightness data and system condition readout. A supervisory computer unit and control distribution bus coupled to control and monitoring points of the processor subsystems make up the core of the system control unit. Control and monitor functions available include: (1) system and subsystem test and calibration and (2) control of normal processing operations using either input data from the radiotelescope or data on previously recorded film frames which are retrievable from a film file.

A hybrid-optical processor system of the type introduced here can provide performance which is both accurate and of high processing speed for VLA radiotelescope data processing. The detailed approach to subsystem and component design can, of course, be varied from that described.

Summary

Basic aspects of very large array radiotelescope output data and its Fourier transform processing have been described. A method for implementation of optical two-dimensional Fourier transform processing of visibility function data has been defined and salient features of the design configuration were presented in the context of the NRAO/Soccarro system.

Acknowledgement is made of very useful discussions with NRAO staff members including J.M. Bulabois, B.G. Clark and L.R. D'Addario during the course of an ERIM study[3] of optical processing methods for radiotelescope data. This study provided the basis for this and companion papers[6,7] on the subject.

References

1. E.B. Fomalont, "Earth Rotation Aperture Synthesis," Proc. of IEEE, Vol. 61, No. 9, September 1973.

2. G.W. Swenson and N.C. Mathur, "The Interferometer in Radio Astronomy," Proc. of IEEE, Vol. 56, No. 12, December 1968.

   R.N. Bracewell, et al., "Giant Radio Galaxies," Scientific American, August 1974.

   J.W.M. Baars, et al., "The Stanford Five-Element Array Radiotelescope," Proc. of IEEE, Vol. 61, No. 9, September 1973.

   R.G. Strom, G.K. Miley, and J. Oart, "The Synthesis Radio Telescope at Westerbork," Proc. of IEEE, Vol. 61, No. 9, September 1973.

   W.N. Christiansen, "A New Southern Hemisphere Synthesis Radio Telescope," Proc. of IEEE, Vol. 61, No. 9, September 1973.

   H.. Ko, "Coherence Theory of Radio-Astronomical Measurements," IEEE Transactions on Antennas, Vol. AP-15, No. 1, January 1967.

3. I. Cindrich, C. Aleksoff, J. Fienup, A. Klooster, and R. Dallaire, "Optical Processor System for VLA Radio Telescope Data," ERIM Report 123400-8-F, April 1977.

4. T.W. Cole, "Holographic Reconstruction of Aperture Synthesis Data," Journal of Optics (Paris), Vol. 9, No. 5, 1978.

5. J.W. Goodman, Introduction to Fourier Optics (McGraw-Hill, San Francisco, 1968).

6. J.R. Fienup and L.E. Somers, "Optical Processor for the VLA Radiotelescope: Encoding-Dependent Errors," SPIE/IEEE International Optical Computing Conference Proceedings, Vol. 231, April 1980.

7. C.C. Aleksoff and L.E. Somers, "Optical Processor for the VLA Radiotelescope: Aberration Analysis," SPIE/IEEE International Optical Computing Conference Proceedings, Vol. 231, April 1980.

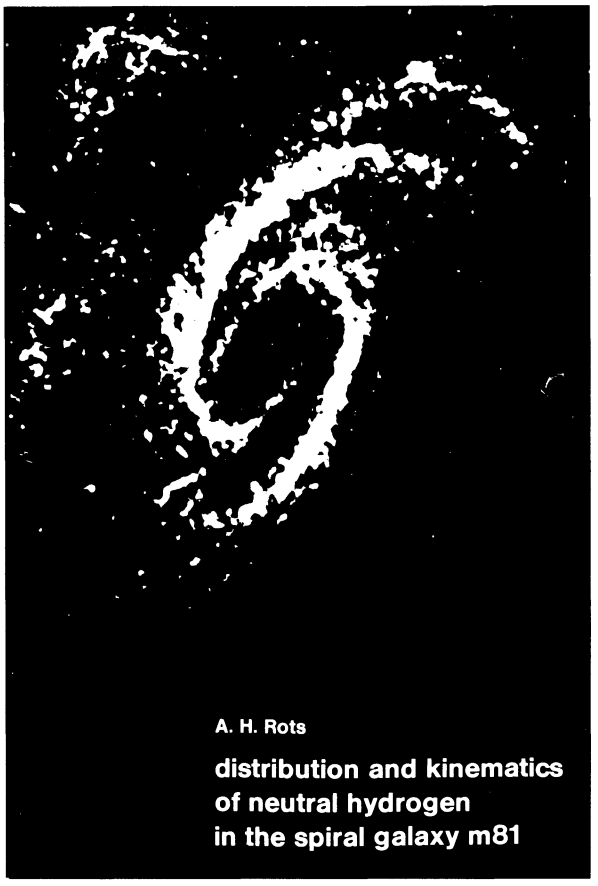

Figure 1. Copy from the Work of A. Rots

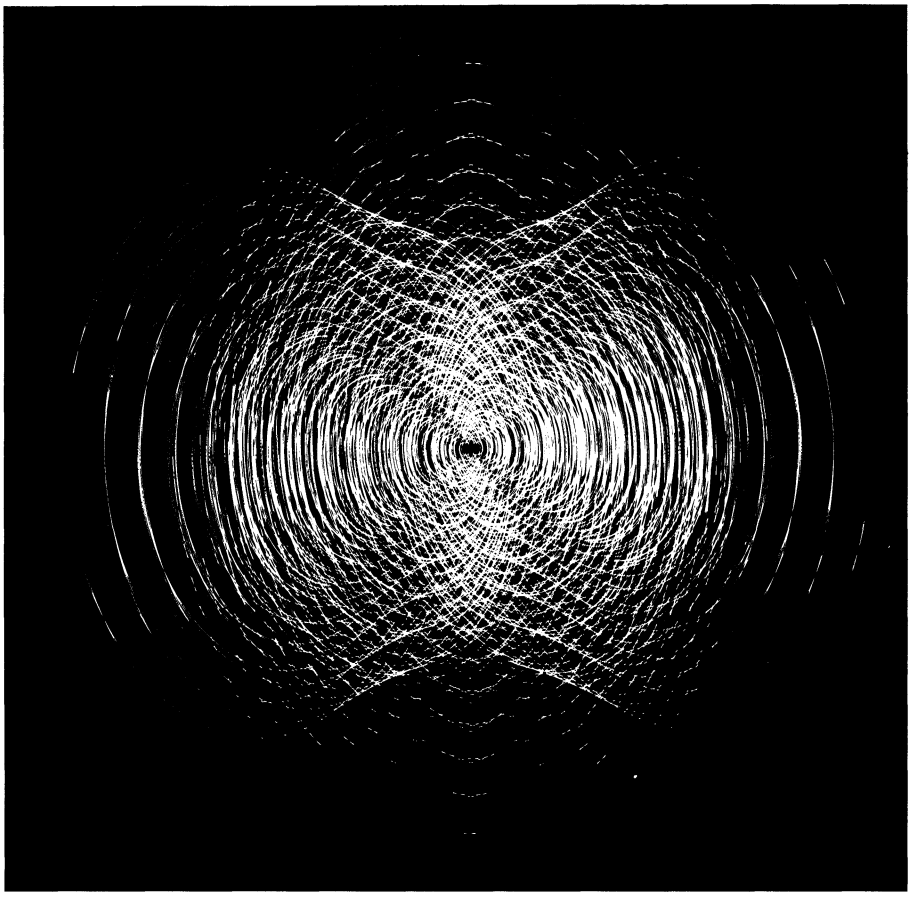

Figure 2. An Example of the Visibility Function (Simulated)

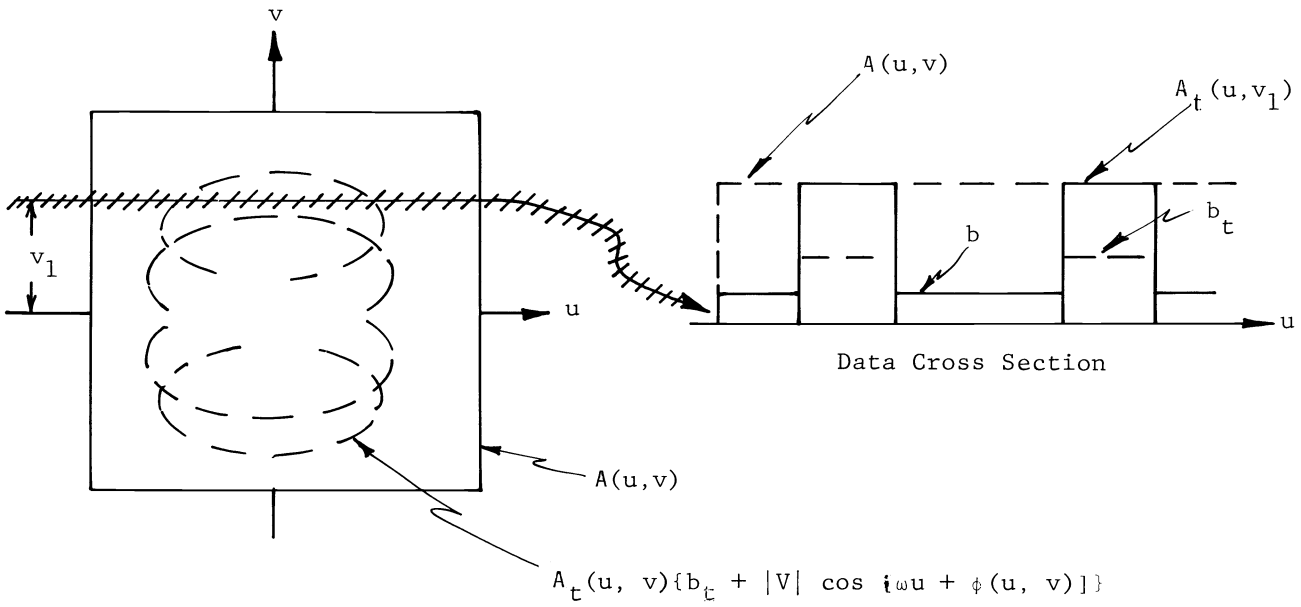

Figure 3. Visibility Function Data Frame Properties

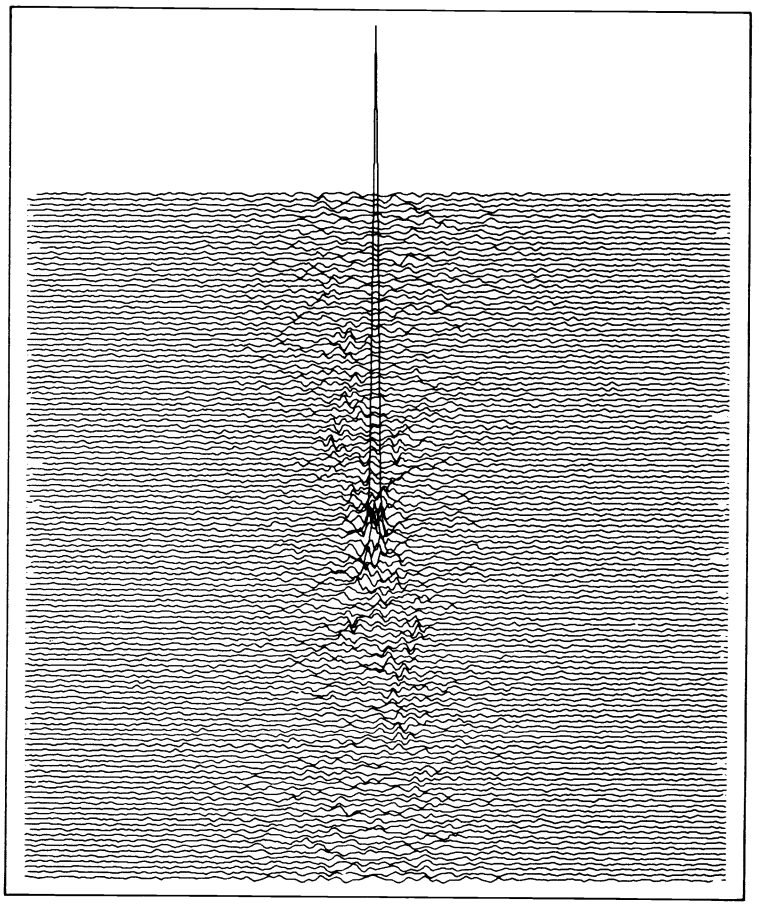

Figure 4. Reconstructed Brightness for a Point Source (Simulated)

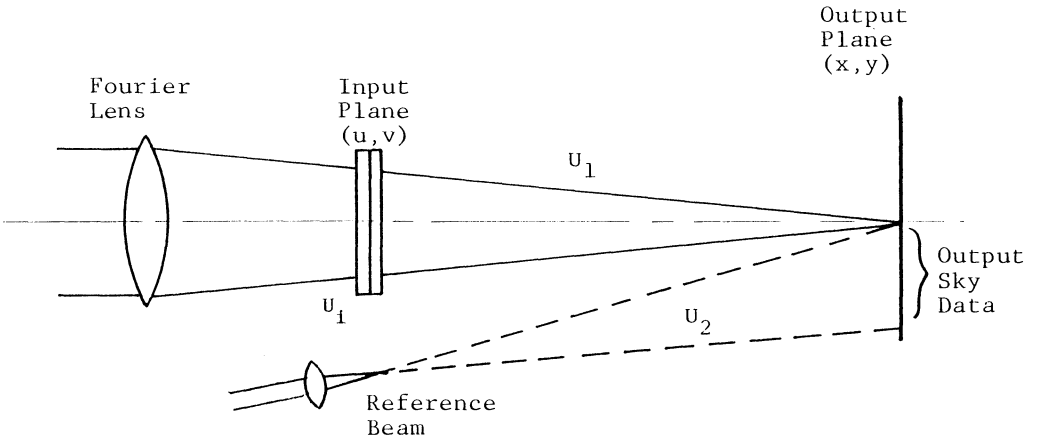

Figure 5. Optical Processing Channel

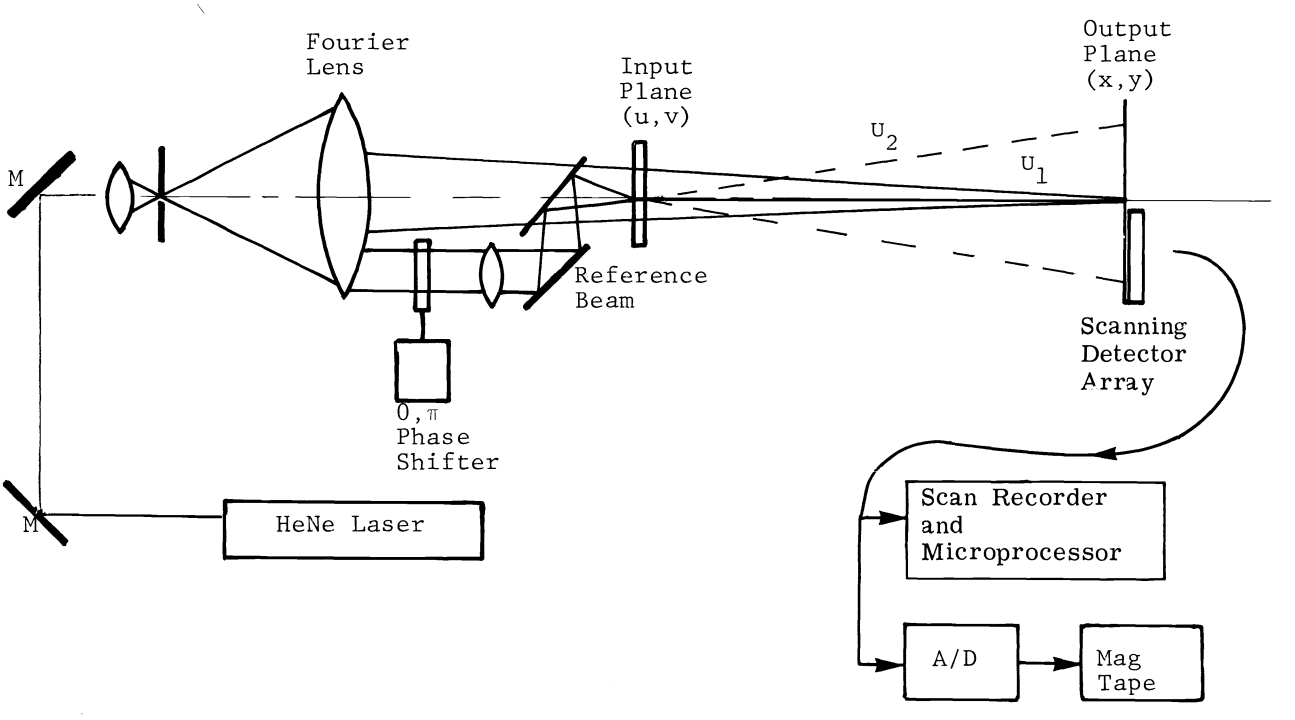

Figure 6. Experimental Optical Processing Channel

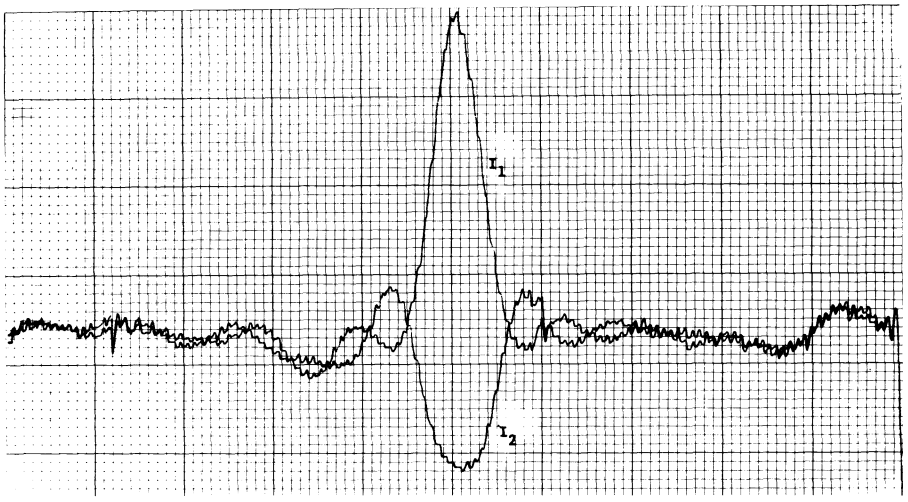

Figure 7a. Individual Scans for I_1 and I_2 at the Processor Output for a Full Circular Input Aperture Containing 10 c/mm Grating

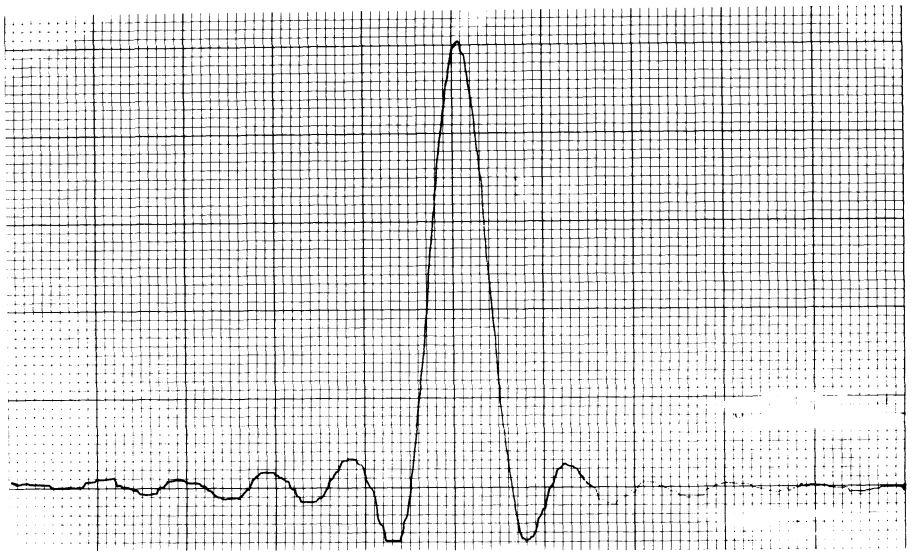

Figure 7b. The Differences of Scans I_1 and I_2 (Full Circular Input Aperature)

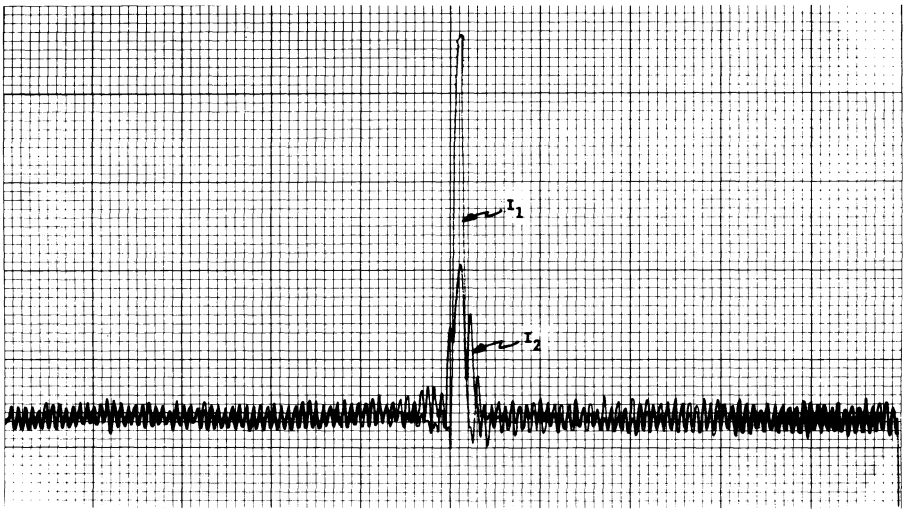

Figure 8a. Individual Scans for I_1 and I_2 at the Processor Output for an Input Visibility Function Having a 10 c/mm Fringe Pattern at the Input Plane (20 mm Square)

Figure 8b. The Difference of Scans I_1 and I_2 (Visibility Function Input)

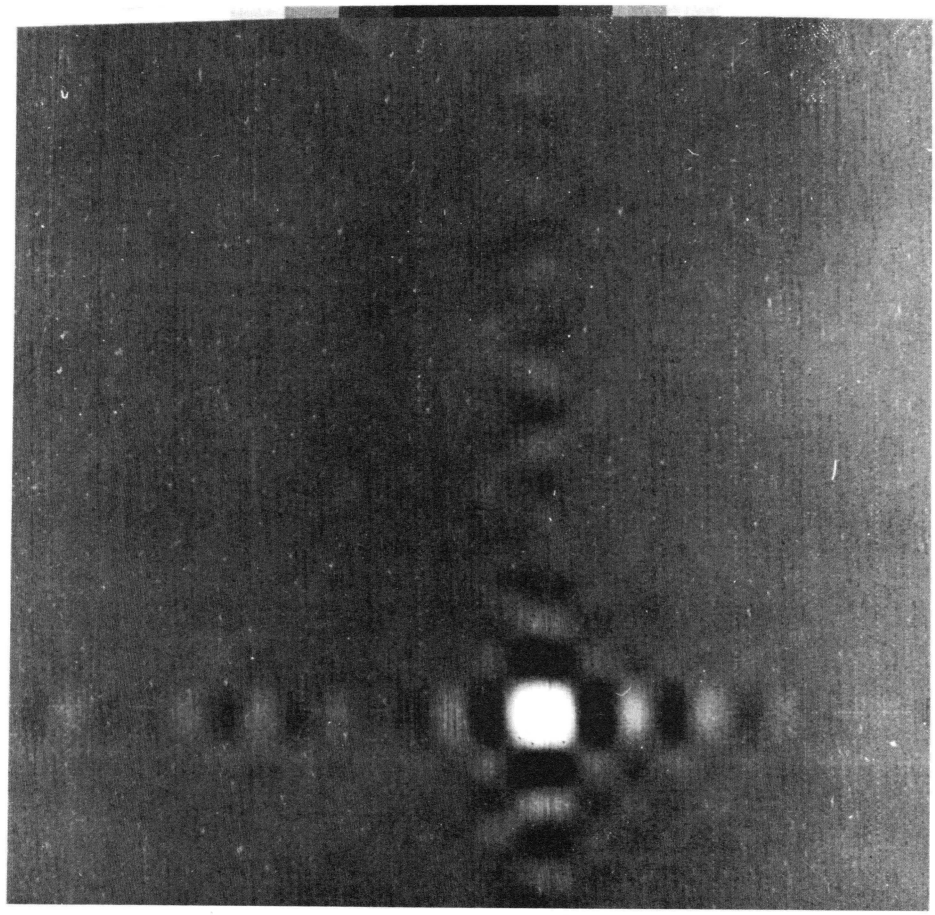

Figure 9. Experimental Processor Output Viewed on a Ramtek TV Display After Photodector Readout and Digitization.

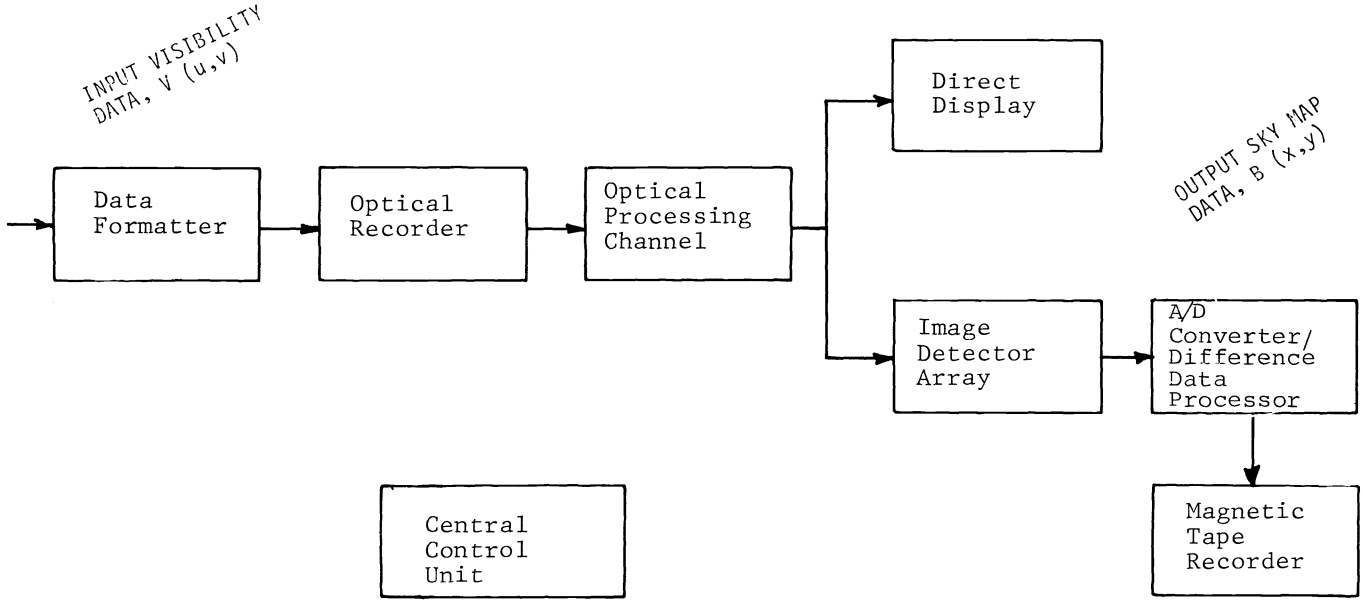

Figure 10. Hybrid-Optical Processor System Concept

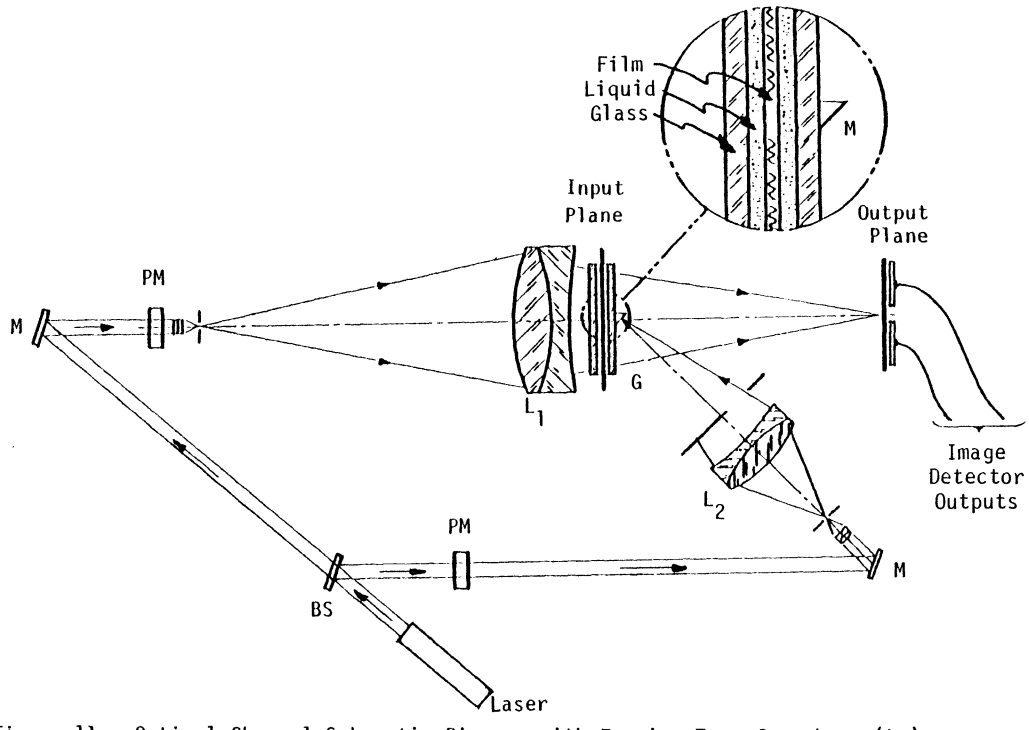

Figure 11. Optical Channel Schematic Diagram with Fourier Transform Lens (L_1), Reference Wave Lens (L_2), Phase Modulators (PM), Mirrors (M), Beamsplitters (BS) and Input Film Liquid Gate (G).